ISSN 1024-8560, Atmospheric and Oceanic Optics, 2015, Vol. 28, No. 2, pp. 185–191. © Pleiades Publishing, Ltd., 2015.
Original Russian Text © V.A. Banakh, I.N. Smalikho, A.V. Falits, B.D. Belan, M.Yu. Arshinov, P.N. Antokhin, 2014, published in Optika Atmosfery i Okeana.

OPTICAL INSTRUMENTATION

Joint Radiosonde and Doppler Lidar Measurements of Wind in the Atmospheric Boundary Layer

V. A. Banakh, I. N. Smalikho, A. V. Falits, B. D. Belan, M. Yu. Arshinov, and P. N. Antokhin

V.E. Zuev Institute of Atmospheric Optics, Siberian Branch, Russian Academy of Sciences, pl. Akademika Zueva 1, Tomsk, 634055 Russia
e-mail: banakh@iao.ru, smalikho@iao.ru, falits@iao.ru, bbd@iao.ru, michael@iao.ru, apn@iao.ru

Received February 11, 2014

Abstract—Results of joint measurements of height profiles of wind velocity and direction by the Stream Line pulse coherent Doppler lidar and RS92-SGP radiosonde in Tomsk from 23 to 27 of September, 2013, are presented. It has been established that wind profiles can be retrieved up to heights from 400 to 1100 m depending on the aerosol concentration in the atmospheric boundary layer from lidar data measured at an elevation angle of 45°. It is shown that the coefficient of correlation between lidar and radiosonde measurements of wind velocity and direction is equal to 0.97. The mathematical expectation and standard deviation of the difference between estimates for the wind velocity and direction from the radiosonde and lidar data amount to 0.1 and 0.7 m/s, respectively, for the velocity and 0.8° and 4°, respectively, for the wind direction.

Keywords: atmospheric boundary layer, wind, coherent Doppler lidar, radiosonde

DOI: 10.1134/S1024856015020025

In recent times, coherent Doppler lidars (CDLs) operating at a wavelength of 1.5 μm (in particular, Stream Line pulse CDL designed and produced by HALO Photonics) gain increasingly greater currency for wind measurements in the boundary air layer [1]. The package of the Stream Line lidar includes a scanning device allowing one to change the propagation direction of the probing pulse and, therefore, to obtain information about wind velocity and direction from raw lidar data. The echo signal level and, consequently, possibilities of obtaining such information are determined in many aspects by aerosol concentration in the atmospheric boundary layer. To study problems concerning the accuracy and maximum range of wind velocity and direction measurements, the Stream Line lidar was involved in the complex lidar experiment carried out in Tomsk in autumn 2013. The experiment also involved radio sounding from the data of which height profiles of different atmospheric parameters (in particular, wind velocity and direction) were retrieved. The description of the experiment and method for retrieving height profiles of wind from lidar data, as well as results of the comparative analysis of joint lidar and radiosonde wind measurement data are presented below.

The experiments were carried out from September 23 to 27, 2013. The lidar was mounted on the roof of the block A building of the Institute of Atmospheric Optics (IAO), Siberian Branch, Russian Academy of Sciences (Fig. 1), and helium-filled balloons for radio sounding were released from the ground near the IAO HARS Station. The distance between the block A and IOA HARS Station is about 430 m. The experiments involved an RS92-SGP radiosonde by Vaisala. The ascension rate of the balloon during the experiments was 5 m/s. Correspondingly, the ascension time of the balloon to the height of 1 km was about 3.5 min. During five days of the experiments, 16 balloons were released. In the same time, measurements by a Stream Line pulse coherent Doppler lidar were carried out. The main parameters of this lidar are presented below.

Wavelength	1.5 μm
Pulse energy	100 μJ
Pulse duration	170 ns
Pulse repetition frequency	15 kHz
Telescope diameter	7.5 cm
Beam radius at the exit of the telescope	2 cm
Focal distance	≥300 m
Minimum measurement range	100 m
Maximum measurement range	0.5–2 km
Bandwidth of the receiver	50 MHz

During the lidar measurements, conical scanning by a probing beam was used. The elevation angle φ of the sounding direction was assigned to be 45°, and one complete conical scanning took about 5 min. The software installed on the computer included in the lidar

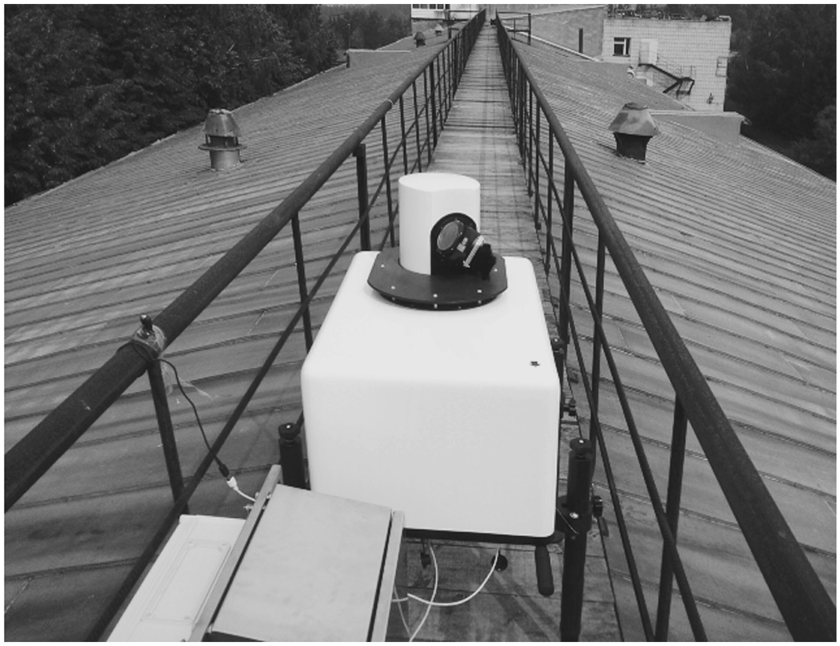

Fig. 1. Stream Line coherent Doppler lidar during experiments on the roof of the IAO building.

package allows one, in addition to specifying measurement parameters (elevation angle, scanning rate, number of probing pulse soundings for accumulation, etc.), to preliminarily process raw lidar data. For the accumulation, we used series of 15000 probing pulses. As a result of this processing, we obtained estimates for the radial velocity $\hat{V}_r$, signal-to-noise ratio $\hat{\mathrm{SNR}}$, and coefficient of aerosol backscatter $\hat{\beta}_\pi$ at different distances from the lidar $R_i = R_0 + i\Delta R$ and at different azimuth angles of scanning $\theta_m = \theta_0 + m\Delta\theta$, where $i = 0, 1, 2, \ldots, I-1$, ΔR is the range resolution, $m = 1, 2, 3, \ldots, M$ and $\Delta\theta$ is the azimuth resolution. Here, $|\theta_M - \theta_0| = 360°$.

Figure 2 shows an example of a lidar measured radial velocity distribution on the lateral surface of the cone of probing beam scanning. It is seen that, beginning from the distance of ~600 m, the probability of a bad estimate of the radial velocity becomes different from zero and the number of bad estimates during one complete scanning increases with an increase in the measurement range R_i. For this reason, to retrieve height profiles of wind velocity $U(h_i)$ and direction angle $\theta_V(h_i)$ (to obtain estimates for wind velocity and direction at heights $h_i = h_L + R_i \sin\varphi$, where h_L is the height of the lidar position point over the Earth's surface) from data similar to those shown in Fig. 2, we applied the filtered sine wave fitting (FSWF) method [2–4].

The essence of the FSWF method is to find the maximum of the filtering function

$$Q(\mathbf{V}) = \frac{100\%}{M}\sum_{m=1}^{M}\exp\left\{-\frac{[\hat{V}_r(R_i,\theta_m) - \mathbf{S}_m\cdot\mathbf{V}]^2}{2\sigma_g^2}\right\}, \quad (1)$$

where $\mathbf{V} = \{V_z, V_x, V_y\}$ is the unknown wind velocity vector; $\mathbf{S}_m = \{\sin\varphi, \cos\varphi\cos\theta_m, \cos\varphi\sin\theta_m\}$ is the unit vector along the direction of the beam; and σ_g is the filtration parameter of good estimates of the radial velocity, i.e., for the estimate of the wind velocity vector $\hat{\mathbf{V}} = \{\hat{V}_z, \hat{V}_x, \hat{V}_y\}$, one can write $Q(\hat{\mathbf{V}}) = \max\{Q(\mathbf{V})\}$. If σ_g is of the order of the Doppler spectrum width (in units of velocity) and the estimate $\hat{\mathbf{V}}$ is obtained with a high accuracy, the maximum of the filtering function $Q(\hat{\mathbf{V}})$ is the percentage of good estimates of the radial velocity among all estimates $\hat{V}_r(R_i, \theta_m)$ obtained during one complete conical scanning by the probing beam at a fixed distance R_i.

Figure 3 shows the retrieval result for height profiles of the velocity $\hat{U} = \left|\hat{V}_x + j\hat{V}_y\right|$, direction angle $\hat{\theta}_V = \arg\{\hat{V}_x + j\hat{V}_y\}$ $(j = \sqrt{-1})$, and vertical component $\hat{V}_z$ of wind from data shown in Fig. 2 using the FSWF method at $\sigma_g = 2$ m/s. The sharp change in wind profiles at a height of about 930 m is related to the significant increase in the number of bad estimates of the radial velocity at this height and in superstratum, when using the filtration procedure in estimating the wind velocity vector does not permit one to obtain the result

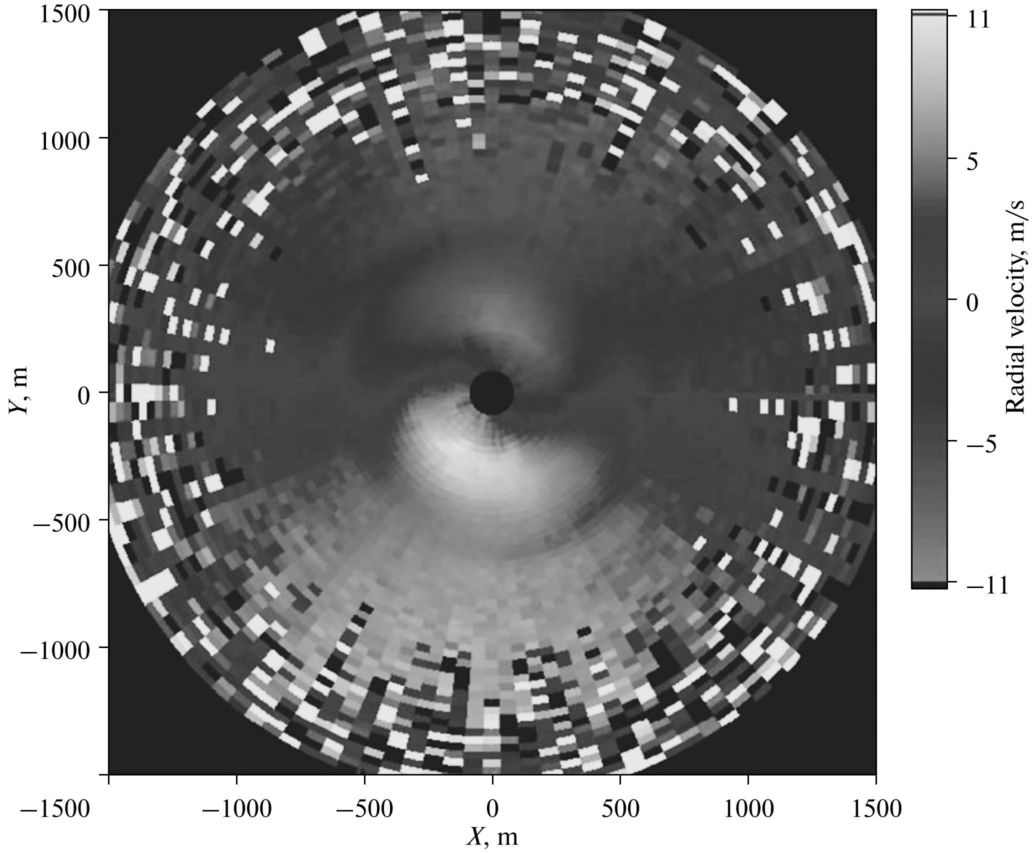

Fig. 2. Distribution of the radial wind velocity on the lateral surface of the scanning cone according to measurements by the Stream Line lidar on September 25, 2013, from 09:00 to 09:05 LT in Tomsk.

with an acceptable accuracy (e.g., when the error of the estimate for velocity does not exceed 0.5 m/s). Therefore, it is necessary to determine the height interval within which retrieval results for wind profiles correspond to the reliable information with a high probability.

The estimate of the radial velocity $\hat{V}_r(R_i,\theta_m)$ is unbiased if the probability of a bad estimate is negligible. Here, the unbiased estimated can be represented in the form [4–7]

$$\hat{V}_r(R_i,\theta_m) = \bar{V}_r(R_i,\theta_m) + V_e(R_i,\theta_m), \quad (2)$$

where $\bar{V}_r$ is the radial velocity averaged over the sounding volume and V_e is a random error possessing the white noise property. i.e.,

$$\langle V_e(R_i,\theta_m)V_e(R_i,\theta_k)\rangle = \langle V_e^2\rangle \delta_{m-k}$$

(δ_m is the Kronecker delta), with $\langle V_e\rangle = 0$ and $\langle \bar{V}_r V_e\rangle = 0$.

In another limiting case, when the probability of a bad estimate is close to unity, $\hat{V}_r(R_i,\theta_m)$ is determined only by the second summand in the right-hand side of formula (2) and, correspondingly, is an biased estimate (regardless of the quantity $\bar{V}_r$, the average value of the estimate for the radial velocity equals zero). Using the lidar data shown in Fig. 2, we obtain height profiles of the signal-to-noise ratio

$$\mathrm{SNR}(h_i) = M^{-1}\sum_{m=1}^{M} \mathrm{S\hat{N}R}(R_i,\theta_m).$$

The error of the lidar estimate of the radial velocity is calculated by the formula

$$\sigma_e(h_i) = \left\{(M-1)^{-1}\sum_{m=1}^{M-1}[\hat{V}_r(R_i,\theta_{m+1}) - \hat{V}_r(R_i,\theta_m)]^2\right\}^{1/2},$$

and the maximum of the filtering function $Q_{\max}(h_i) \equiv Q(\hat{\mathbf{V}}(h_i))$. Here, one should note that, in the case of an unbiased estimate $\hat{V}_r(R_i,\theta_m)$ (see formula (2)), the calculated quantity σ_e somewhat exceeds the real error $\left[\langle V_e^2\rangle\right]^{1/2}$ due to the wind turbulence (since $\langle[\bar{V}_r(R_i,\theta_{m+1}) - \bar{V}_r(R_i,\theta_m)]^2\rangle \neq 0$).

The calculation results for $\mathrm{SNR}(h_i)$, $\sigma_e(h_i)$, and $Q_{\max}(h_i)$ are shown in Fig. 4.

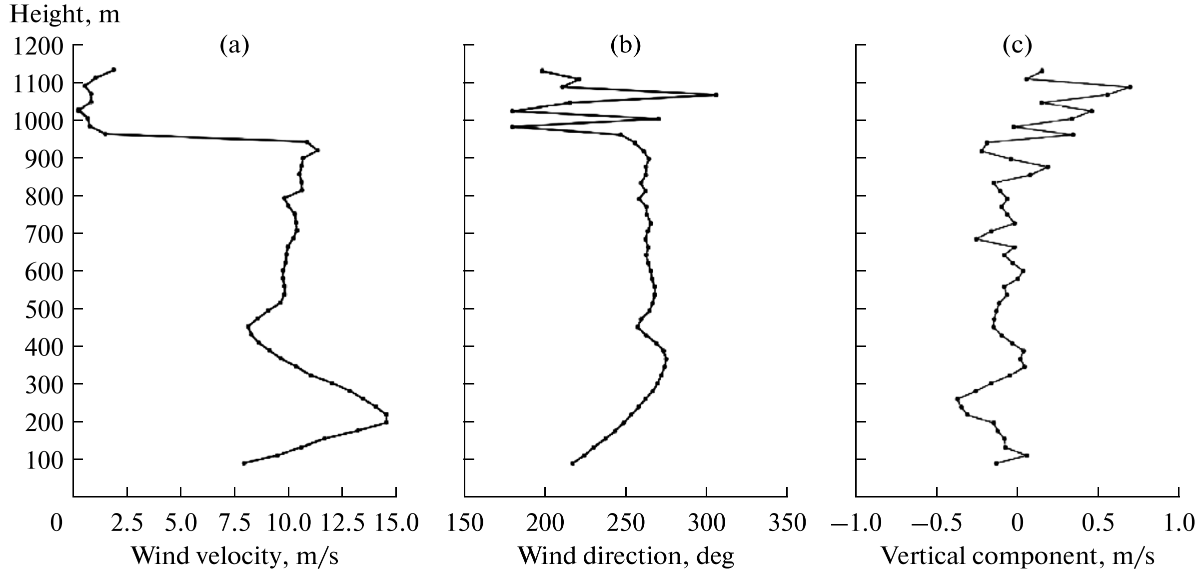

Fig. 3. Height profiles retrieved using the FSWF method from the data shown in Fig. 2 for (a) velocity, (b) direction, and (c) vertical component of wind.

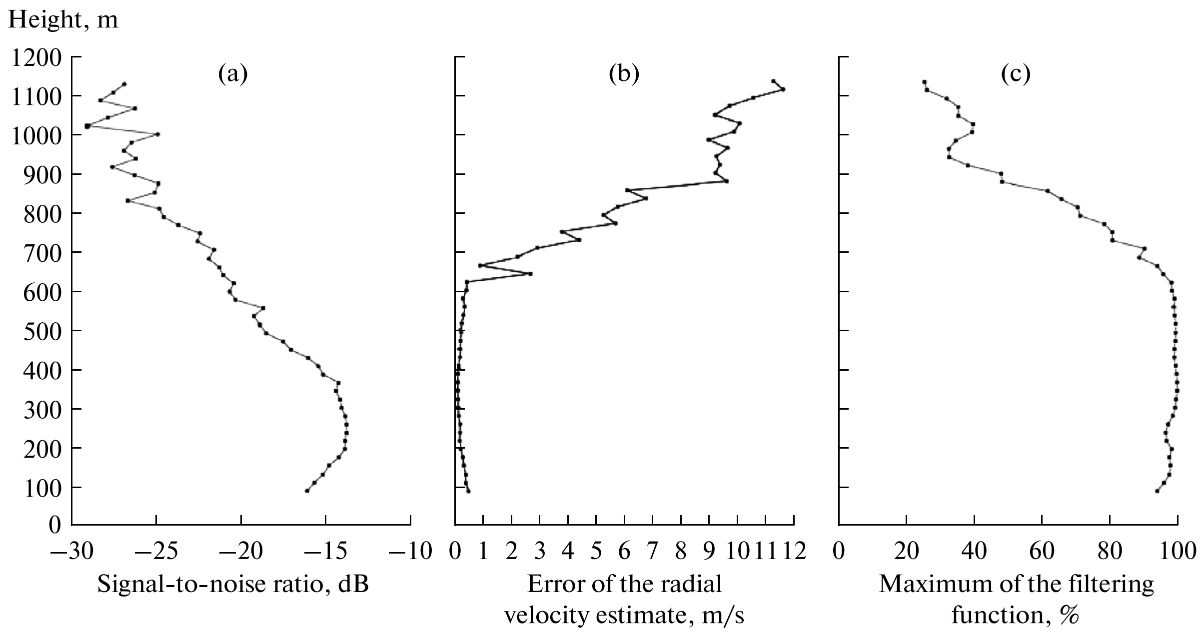

Fig. 4. Height profiles obtained from the data shown in Fig. 2 for the (a) signal-to-noise ratio, (b) error of the estimate of the radial velocity, and (c) maximum of the filtering function.

It is seen that below the height of 600 m, when the signal-to-noise ratio is greater or equal to −21 dB, the radial velocity estimate, wherein the error σ_e does not exceed 0.5 m/s (Fig. 4b), is unbiased because the maximum of the filtering function $Q_{\max}$ is close to 100% (Fig. 4c). With an increase in height $h > 600$ m, σ_e increases and $Q_{\max}$ decreases (due to an increase in the number of bad estimates of the radial velocity) and, correspondingly, the estimate of the radial velocity becomes biased [4]. Nevertheless, using the FSWF method allows one to obtain an unbiased estimate for the wind velocity vector at heights of up to 900 m. Here, the maximum of the filtering function $Q_{\max}$ does not go below 40%. Therefore, to retrieve altitude profiles of wind with an acceptable accuracy (the error in the estimate for wind velocity must not exceed 0.5 m/s), the condition $Q_{\max} \geq 40\%$ must be satisfied for the maximum height of the retrieved wind profiles.

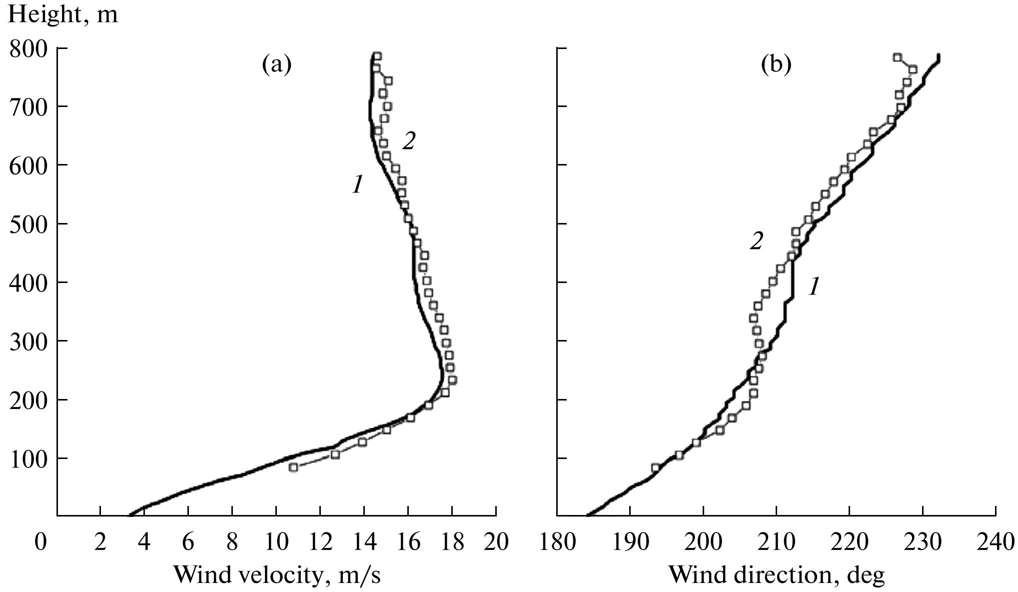

Fig. 5. (a) Wind velocity and (b) wind direction height profiles retrived from data of radiosonde and lidar measurements in Tomsk on September 24, 2013, at 22:30 LT: radiosounding (*1*) and lidar data (*2*).

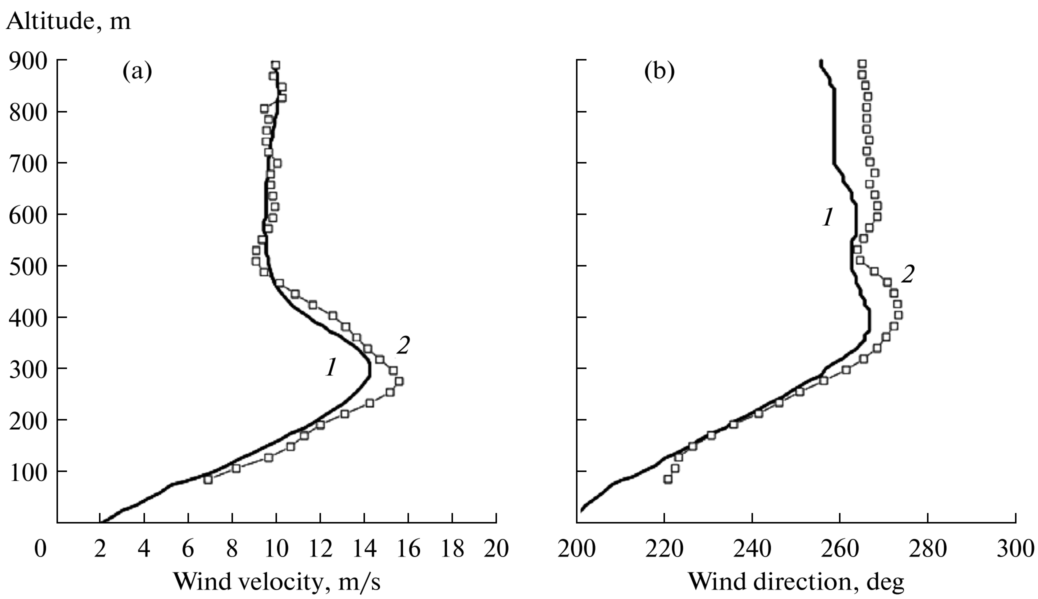

Fig. 6. (a) Wind velocity and (b) wind direction height profiles retrieved from data of radiosonde and lidar measurements in Tomsk on September 25, 2013, at 08:30 LT: radiosounding (*1*) and lidar data (*2*).

It is the criterion that was used in retrieving all height profiles of wind from lidar data which were then compared with results of radiosonde measurements.

Figures 5–7 show examples of height profiles of wind velocity and direction; the profiles were obtained from data of joint radiosonde and Doppler lidar measurements in Tomsk in autumn, 2013. In these examples, the maximum height of wind profile retrieval from data measured by the Stream Line lidar is 800 (Fig. 5), 900 (Fig. 6), and 600 m (Fig. 7). One can see a quite satisfactory agreement between measurement results obtained by two different methods up to these heights selected by the above criterion ($Q_{max} \geq 40\%$).

The height profiles of wind velocity and direction were retrieved with a height resolution $\Delta h = 21.2$ m from lidar data and $\Delta h \sim 10$ m from radiosounding data. The maximum height of wind profile retrieval from lidar data significantly depends on concentration of atmospheric aerosol and, according to exper-

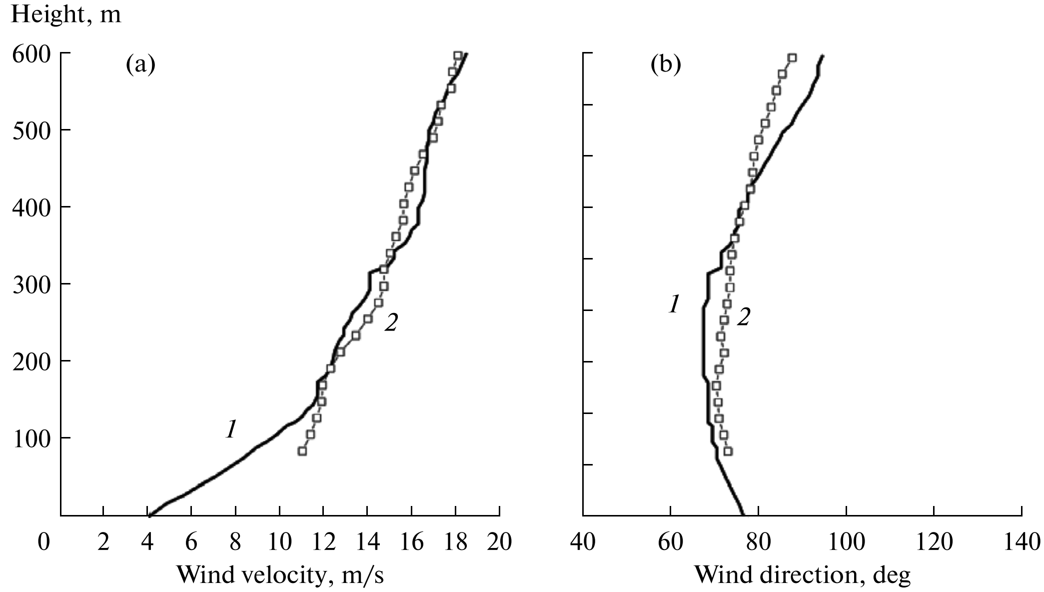

Fig. 7. (a) Wind velocity and (b) wind direction height profiles retrieved from data of radiosonde and lidar measurements in Tomsk on September 26, 2013, at 18:00 LT: radiosounding (*1*) and lidar data (*2*).

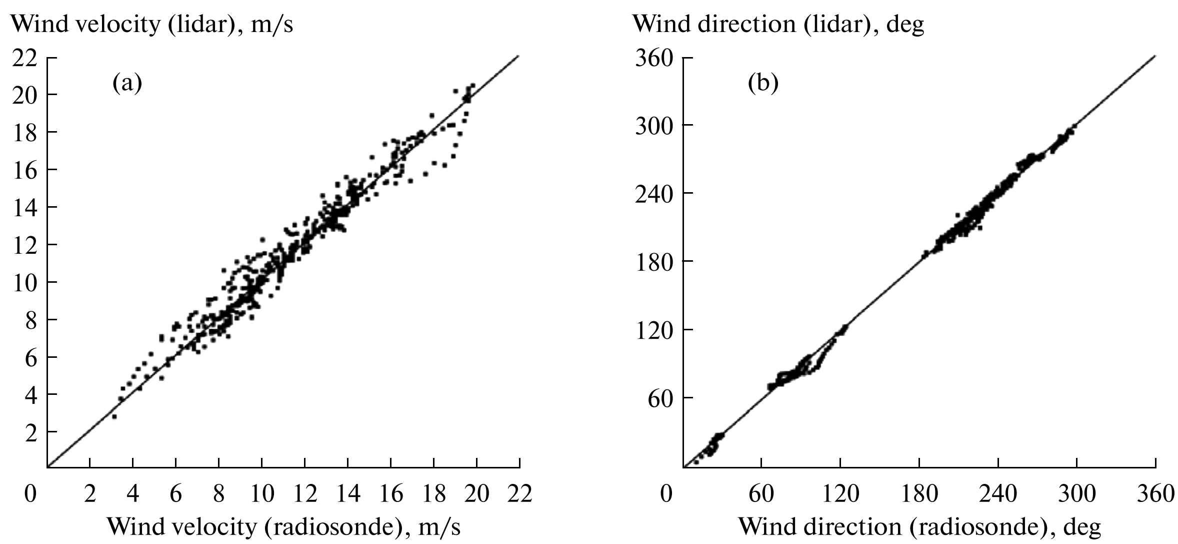

Fig. 8. Comparison of (a) wind velocity and (b) wind direction estimates (dots) obtained from data of joint radiosonde and lidar measurements in Tomsk on September 23–27, 2013.

iments, takes values from 400 to 1100 m at an elevation angle of 45°.

Figure 8 shows in the form of dots all individual estimates of wind velocity and direction from data of joint radiosounding and lidar measurements at corresponding heights during experiments from September 23 to 27, 2013. The statistical analysis of these results shows that the coefficient of correlation between radiosonde and lidar estimates of wind velocity and direction is equal to 0.97. The mathematical expectation and standard deviation of the difference between estimates of wind velocity and direction from the radiosonde and lidar data are 0.1 and 0.7 m/s, respectively, for the velocity and 0.8° and 4°, respectively, for the direction.

Thus, the above results of joint radiosonde and Doppler lidar measurements point to high efficiency of using the Stream Line lidar for obtaining operational and reliable information about the height behavior of wind velocity and direction and extend the range of problems of laser sounding of the atmosphere [8, 9]. Applying the FSWF method for processing wind data (radial velocities) measured by this lidar permits one in most cases to retrieve vertical profiles of components of the wind velocity vector almost in the entire atmospheric boundary layer (up to height of a ~1 km). In the future, we plan to carry out theoretical and experimental investigations of the possibility to extract information about atmospheric turbulence from data measured by the Stream Line lidar.

ACKNOWLEDGMENTS

This work was supported in part by the Russian Foundation for Basic Research (project no. 13-05-00458).

REFERENCES

1. G. Pierson, F. Davies, and C. Collier, "An analysis of performance of the UFAM Pulsed Doppler lidar for the observing the boundary layer," J. Atmos. and Ocean. Technol. **26** (2), 240–250 (2009).
2. I. N. Smalikho, "Techniques of wind vector estimation from data measured with a scanning coherent Doppler lidar," J. Atmos. and Ocean. Technol. **20** (2), 276–291 (2003).
3. V. A. Banakh, A. Brewer, E. L. Pichugina, and I. N. Smalikho, "Measurements of wind velocity and direction with coherent doppler lidar in conditions of a weak echo signal," Atmos. Ocean. Opt. **23** (5), 333–340 (2010).
4. V. A. Banakh and I. N. Smalikho, *Coherent Doppler Wind Lidars in a Turbulent Atmosphere* (Artech House, Boston; London, 2013).
5. R. G. Frehlich, "Estimation of velocity error for Doppler lidar measurements," J. Atmos. and Ocean. Technol. **18** (10), 1628–1639 (2001).
6. R. G. Frehlich and L. B. Cornman, "Estimating spatial velocity statistics with coherent Doppler lidar," J. Atmos. and Ocean. Technol. **19** (3), 355–366 (2002).
7. V. A. Banakh and I. N. Smalikho, "Estimation of the turbulence energy dissipation rate from the pulsed Doppler lidar data," Atmos. Ocean. Opt. **10** (12), 957–965 (1997).
8. G. G. Matvienko and V. A. Pogodaev, "Atmospheric and ocean optics as uncompleted task of interaction of optical radiation with a propagation medium," Opt. Atmos. Okeana **25** (1), 5–10 (2012).
9. I. A. Razenkov, "Aerosol lidar for continuous atmospheric monitoring," Atmos. Ocean. Opt. **26** (1), 52–63 (2013).

Translated by A. Nikol'skii